



# Ruthenium (II) $\beta$ -diketimine as hydroamination catalyst, crystal structure and DFT computations

Sara Dindar<sup>1</sup> · Ali Nemati Kharat<sup>1</sup> · Barzin Safarkoopayeh<sup>1</sup> · Alireza Abbasi<sup>1</sup>

Received: 21 November 2020 / Accepted: 19 March 2021  
© The Author(s), under exclusive licence to Springer Nature Switzerland AG 2021

## Abstract

A new half-sandwich ruthenium (II) complex containing  $\beta$ -diketiminate ligand has been synthesized and used for hydroamination of acrylonitrile with aromatic and aliphatic amines. The catalytic activity of prepared complex was compared with a series of ruthenium complexes of  $\beta$ -diketiminate ligands, and the effect of electronic and steric properties of these ligands on catalytic activity of their complexes was investigated. Replacement of H atom in  $\alpha$  position of  $\beta$ -diketiminate with (CF<sub>3</sub>) as an electron-withdrawing group leads to decreasing the reaction yield, and on the other hand, electron-donating group (CH<sub>3</sub>) has the opposite effect. In addition, crystal structure of [Ru(*p*-cymen)Cl(L<sup>H,Cl</sup>)] was determined by single X-ray crystallography. Hirshfeld surface analysis has been performed to determine the dominate interactions in molecular crystal. Furthermore, density functional, QTAIM and energy calculations have been carried out, to get the detailed insight into electronic and bonding characteristics of titled compound.

## Introduction

Amines are commonly found as fundamental compounds in the bulk and fine chemical industry since they are widely used in agrochemicals, dyes, natural products and pharmaceutically active compounds [1]. Numerous methods have been developed for synthesis of amines such as N-alkylation of amines with alkyl and aryl halides, amination of carbonyl compounds and amination of alcohols [2–5]. Addition of an N–H group from a nucleophilic amine or ammonia directly to a C–C multiple bond known as hydroamination reaction has received extensive attention because of 100% atom-efficient process, broad availability and low-cost starting materials [6]. Due to the thermodynamic characteristics of this transformation (weakly exergonic and highly negative entropy), using an applicable catalytic system is essential [7]. Various types of transition metal complexes, the lanthanides, the alkaline earth metals and strong bases have been utilized as the catalysts for hydroamination reactions [8–15].

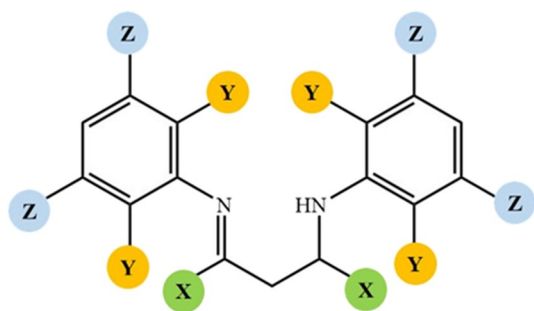
Applying late transition metals for selective preparation of amines by hydroamination reaction has been reported in several research papers [6]. Kozlov in 1936 reported the

addition of aniline to acetylene in the presence of mercury (II) chloride as the first homogenous system for hydroamination of alkynes [16]. Subsequently, many catalytic systems by transition metals, such as palladium, rhodium, nickel and ruthenium have been shown to provide acceptable catalytic activity [17–20]. Ruthenium complexes show strong activity in coordination and activation of unsaturated C–C bonds, so these complexes are used extensively as catalysts in some transformations, such as olefin metathesis, C–H activation and hydrogenation [21–24]. Among these ruthenium complexes, half-sandwich ruthenium (II) complexes coordinated to  $\eta^6$ -arenes are well developed and have a wide range of applications as catalyst precursors. Shibata et al. reported the first enantioselective hydroamination of styrene with secondary alkylamines in the presence of [Ru(benzene)Cl<sub>2</sub>]<sub>2</sub>, in which the asymmetric anti-Markovnikov products were generated in moderate yields [25, 26].

Among half-sandwich arene–ruthenium complexes, the products containing dinitrogen ligands have been extensively investigated and shown excellent activities in a wide range of catalytic reactions, such as reduction of ketones and imines, leading to secondary alcohols and amines [27]. The  $\beta$ -diketiminate ligands known as “nacnac” are chelating bidentate ligands, with a framework according to Scheme 1, which have gained considerable attention in stabilizing transition-metal complexes in regard of diverse coordinating modes and tunable stereo-electronic features. Coordination

✉ Ali Nemati Kharat  
anemati@ut.ac.ir

<sup>1</sup> School of Chemistry, College of Science, University of Tehran, Tehran, Iran



**Scheme 1** Typical  $\beta$ -diketiminato framework (nacnac ligands were specified as  $L_o^{X,Y}$  and  $L_m^{X,Z}$  in text)

chemistry of nacnac ligands by the first row transition metals has been investigated comprehensively in comparison with other d-block elements such as Rh, Ir, Pd, Pt and Ru, which have been reported in some publications [28–32].

The half-sandwich arene–ruthenium complexes having various  $\beta$ -diketiminato ligands developed by Phillips et al. efficiently catalyze the addition of  $\text{CCl}_4$  or toluenesulfonyl chloride to styrene. Moreover, the effects of electron-withdrawing and electron-donating groups in the structure of “nacnac” ( $X$  symbols in Scheme 1) on catalyst activation were investigated. Interestingly, the complexes with methyl substituent on the  $\beta$ -diketiminato ligand were almost inactive toward the addition of  $\text{CCl}_4$  to styrene, whereas those having electron-withdrawing  $\text{CF}_3$  substituent showed appreciably high activity [33]. Schreiber and co-workers prepared ruthenium (II) complexes based on fluorinated  $\beta$ -diketiminato ligands and explored their catalytic applicability toward Diels–Alder reactions. These were found to be robust Lewis acid catalysts for the Diels–Alder reaction between  $\alpha,\beta$ -unsaturated aldehydes and dienes [34].

Herein, a new half-sandwich ruthenium (II) complex containing  $\beta$ -diketiminato ligand has been synthesized as it was shown in Scheme 2, and its catalytic activity in hydroamination reactions of aromatic and aliphatic amines with acrylonitrile was investigated. Catalytic activity of other ruthenium complexes consisting of different derivatives of  $\beta$ -diketiminato ligands was compared to our prepared new complex in this reaction. A suitable crystal of prepared  $[\text{Ru}(p\text{-cymen})\text{Cl}(\text{L}^{\text{H,Cl}})]$  complex (complex **1**) was studied by single-crystal X-ray diffraction technique. Results

demonstrate that the structure of the complex is similar to previously reported ruthenium (II)  $\beta$ -diketiminato complexes [35], as Ru(II) has three-coordinate piano-stool geometry. Furthermore, to get insight into the electronic structure of the complex, DFT and QTAIM (Quantum Theory of Atoms in Molecules) calculations were carried out and the electronic structure of the title compound was investigated.

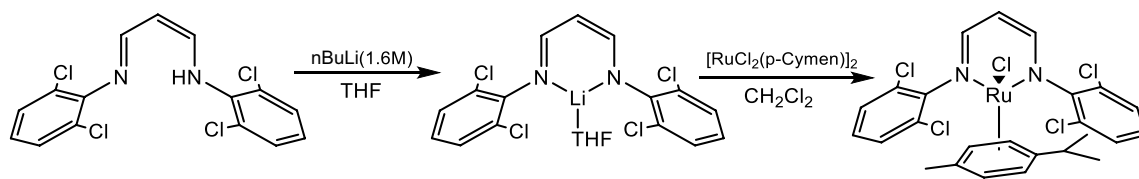
## Computational details

To get insight into the electronic structure of the complex, density functional calculations were carried out with ORCA.4.2.1, using the BP86 functional and the def2-TZVP basis set [36]. The electronic structure of the title compound was investigated by QTAIM (Quantum Theory of Atoms In Molecules) using Multiwfn program [37].

## Experimental

### General

All reactions were performed under nitrogen atmosphere using a nitrogen-filled glove box or standard Schlenk techniques. All the chemicals and reagents used in this study were purchased from Sigma-Aldrich and Strem Chemicals and utilized without purification. The solvents were of analytical grade and purified prior to use based on standard methods.  $[\text{Ru}(p\text{-cymene})\text{Cl}_2]_2$ ,  $\text{RuCl}_2\text{PPh}_3$ ,  $(\text{Cp})\text{RuCl}(\text{PPh}_3)_2$ ,  $\text{RuH}_2(\text{CO})(\text{PPh}_3)_3$  and  $\text{RuCl}(\text{OAc})(\text{PPh}_3)_3$  were prepared according to previously published methods [38–41]. Ruthenium  $\beta$ -diketiminato complexes were used in this study prepared by reported methods in Phillips group [35, 42].  $^1\text{H}$  NMR spectra data were recorded at room temperature in  $\text{CDCl}_3$  on a Bruker AV III HD 400 MHz instrument. Single-crystal X-ray diffraction data were collected with a Bruker X8 APEX II CCD equipped with  $\text{MoK}\alpha$  radiation at room temperature. The course of the reactions was monitored with a gas chromatograph (Agilent Technologies 7890A Instrument), equipped with a capillary column (HP-5, 5% phenyl methyl siloxane, capillary 60.0 mm 9 250 mm 9 1.00 mm) and a flame ionization detector (FID).



**Scheme 2** Synthesis route for preparation of the  $\beta$ -diketiminato- $(\eta^6\text{-arene})\text{-Ru(II)}$  Complex (**1**)

## Catalyst preparation

### Synthesis of $\beta$ -diketiminate ligand $L^{H,Cl}$

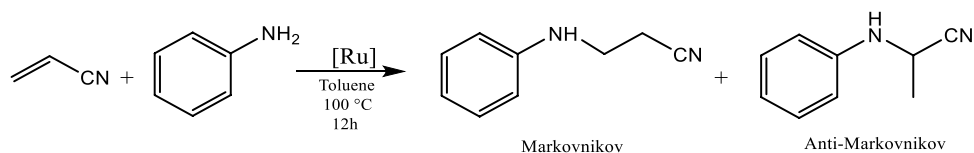
4.5 gr (28 mmol), 2,6-dichloroaniline was added to a solution of 1 ml (13.75 mmol) malondialdehyde in 70 ml toluene. The mixture was heated, and then (0.1 g) *p*-toluenesulfonic acid was added. Afterwards, the reaction was refluxed for 24 h to achieve a clear light yellow solution. Then, solvent was removed under vacuum to get a solid residue. It was dissolved in 40 ml diethyl ether and then quenched with saturated sodium bicarbonate (30 ml), and it was stirred for 1 h at room temperature. Organic layer was separated and dried over  $Na_2SO_4$ , diethyl ether was removed by rotary evaporator, and remaining solid was dried in oven.  $^1H$  NMR (500 MHz,  $CDCl_3$ )  $\delta$ (ppm): 11.84 (*d*, 1H, NH), 7.36 (*t*, H), 6.89 (*d*, 2H,  $\alpha$ -CH), 6.26 (*t*, 2H, Ar-*p*-H) 4.88 (*t*, 1H,  $\beta$ -CH).

### Synthesis of Ruthenium $\beta$ -diketiminate complex $[Ru(p\text{-cymen})Cl(L^{H,Cl})]$

A 0.2 g (0.54 mmol) portion of  $L^{Cl,H}$  was added to a dried 25-mL Schlenk flask under inert conditions. A 20 ml dried and nitrogen-saturated THF was added. The solution was cooled in an ice bath for 10 min, and then 0.5 ml of a 1.6 M *n*-BuLi was added dropwise and the color of the solution changed immediately to yellow. The reaction was stirred at ice bath for 2 h and at room temperature overnight afterwards. Volatile components were removed in vacuum, leaving a bright yellow solid.

In glove box, 0.2 g (0.45 mmol) of  $L^{Cl,H}.Li(THF)$  was dissolved in dried and degassed dichloromethane, and then this suspension was added dropwise to a solution of 70 mg (0.5 equiv.) of  $[RuCl_2(p\text{-cymen})]_2$  in 10 ml  $CH_2Cl_2$ . The reaction mixture was stirred overnight, then precipitated LiCl was removed by filtration, and the solvent was removed in vacuum. After drying under vacuum, a dark red solid was obtained (Scheme 2). Crystals suitable for X-ray diffraction analysis were grown in the mixture of dichloromethane and pentane in  $-30^\circ C$ .  $^1H$  NMR (500 MHz,  $CDCl_3$ )  $\delta$ (ppm): 7.37 (*t*, 4H, Ar-*m*-H), 7.63 (*d*, 2H,  $\alpha$ -CH), 7.15 (*d*, 2H, Ar-*p*-H), 5.71 (*t*, 1H,  $\beta$ -CH), 2.76 (*m*, 1H, *p*-cymene *iPr*-(CH)), 1.70 (*s*, 1H, *p*-cymene  $CH_3$ ), 1.17 (*d*, 6H, *p*-cymene *iPr*-( $CH_3$ )<sub>2</sub>).

**Scheme 3** Hydroamination of acrylonitrile with aniline



## General procedure for the hydroamination

The autoclave was charged with catalyst  $[Ru(p\text{-cymen})Cl(LH,Cl)]$  (0.05 mmol), amine (5 mmol), acrylonitrile (6 mmol) and 1.5 ml toluene as solvent. 0.04 g  $K_2CO_3$  used as base. The autoclave was flushed with argon for 5 min, and then it was stirred at  $100^\circ C$  (Scheme 3). After 20 h, the autoclave was cooled to room temperature and the products were analyzed by gas chromatography (GC). Conversions were calculated for acrylonitrile using *n*-decane as standard.

## Result and discussion

Applying acrylate as an activated olefin in mild condition catalytic hydroamination reaction in the presence of transition metal complexes was reported by different groups of researchers and provided excellent activity. In this work, hydroamination reaction of acrylonitrile with a range of aliphatic amines and aniline in the presence of catalytic amount of half-sandwich ruthenium  $\beta$ -diketiminate complex  $[Ru(p\text{-cymen})Cl(L^{H,Cl})]$  was carried out with selectivity up to 99%. As it can be observed from Table 1, the presence of ruthenium complexes as a catalyst has a significant impact on the reaction yield, especially when complexes with a free coordination site on metal center have been used.

Among the selected catalysts, four-coordinated complex (1) (entry 3) and  $[RuCl_2(p\text{-cymen})]_2$  complex (entry 4)

**Table 1** Hydroamination of acrylonitrile with aniline in the presence of different ruthenium catalysts

No	Catalyst	Conversion (%) <sup>a</sup>	Selectivity <sup>b</sup>
1	No Catalyst	10	–
2	$RuCl_3 \cdot xH_2O$	30	28
3	$[Ru(p\text{-cymen})Cl(L^{H,Cl})]$	98	95
4	$[Ru(p\text{-cymene})Cl_2]_2$	87	85
5	$RuCl_2(PPh_3)_3$	55	50
6	$(Cp)RuCl(PPh_3)_2$	70	60
7	$RuCl(OAC)(PPh_3)_3$	35	28
8	$RuH_2(CO)(PPh_3)_3$	29	25

Acrylonitrile (6 mmol), aniline (5 mmol), catalyst (3 mol%),  $K_2CO_3$  (0.05 mmol), toluene (1 ml),  $T = 100^\circ C$ , 20 h.

<sup>a</sup>Data were determined by GC, and conversions were calculated for acrylonitrile using *n*-decane as standard,

<sup>b</sup>Selectivity is measured for Markovnikov product (Scheme 3)

showed significant activity by conversion of 98% and 87%, respectively. Moreover, six-coordinated  $[\text{RuH}_2(\text{CO})(\text{PPh}_3)_3]$  (entry 8) and  $[\text{RuCl}(\text{OAC})(\text{PPh}_3)_3]$  (entry 7) complexes showed less activity in the reaction conditions. It is proposed that the low reactivity of such saturated metal complexes is caused by an energy-consuming preliminary ligand dissociation.

Reaching acceptable activity from  $[\text{Ru}(\text{p-cymen})\text{Cl}(\text{L}^{\text{H,Cl}})]$  complex (**1**), the effect of ligand architecture was investigated on catalytic activity by testing different ruthenium nacyclopentadienyl complexes which have electron-withdrawing group ( $\text{CF}_3$ ) or electron-donating group ( $\text{CH}_3$ ) in their structure. The monoanionic  $\beta$ -diketiminate ligand provided a robust framework with relatively strong donating properties by bidentate coordination around the metal center. The electronic and steric effect of ligand on metal can be easily tuned by a substituted group on its backbone. Normally, the electronic properties of ligand are affected by group on  $\alpha$  position ( $X$ ) and the steric properties of ligand can be controlled by substituents on ortho position of flanking aryl rings ( $Y$ ) (Scheme 1). To investigate such electronic and steric effects on catalytic activity of  $\beta$ -diketiminate derivatives complexes, a series of these complexes were synthesized according to the instruction that was reported previously [34, 35, 42], and their catalytic activity was compared to a new  $[\text{Ru}(\text{p-cymen})\text{Cl}(\text{L}^{\text{H,Cl}})]$  complex (**1**) that was prepared in this article. As it can be observed from Table 2, these series of complexes show different catalytic activities in reaction condition. In the case of applying  $[\text{Ru}(\text{p-cymen})\text{Cl}(\text{L}^{\text{H,Cl}})]$  complex (**1**), it is proved to be highly efficient as a catalyst for the hydroamination in comparison to other mentioned  $\beta$ -diketiminate complexes. The  $[\text{Ru}(\text{C}_6\text{H}_6)\text{Cl}(\text{L}^{\text{CF}_3, \text{CH}_3})]$ , which carries the electron-withdrawing  $\text{CF}_3$   $X$ -substituent group, showed significantly less activity. In contrast, the presence of electron-donating  $\text{CH}_3$  group in this position leads to higher catalytic activity of complex  $[\text{Ru}(\text{C}_6\text{H}_6)\text{Cl}(\text{L}_\text{O}^{\text{CH}_3, \text{CH}_3})]$  (entry 3). However, the existence of hydrogen in the same place has a moderate electron-donating effect and shows high activity (entry 2). The steric features of ligand also have influence on catalytic activity of complex.

It seems the larger  $\text{CH}_3$  substituent on  $Y$ -position of ligand as it is shown in Scheme 1, making a barrier for active site of complex, and thus a lower rate of reaction was observed for  $[\text{Ru}(\text{C}_6\text{H}_6)\text{Cl}(\text{L}_\text{O}^{\text{CH}_3, \text{CH}_3})]$  (entry 3) in comparison to H substituent in complex  $[\text{RuCl}(\text{L}^{\text{CH}_3, \text{H}})]$  (entry 2). No significant distinction in catalytic activity was observed when substituent on the flanking aryl groups ( $Z$ ) changes from 3,5-dimethyl to trifluoromethyl (entry 5 and 6), so these complexes showed similar activity.

Solvent as one of the important factors can affect the conversion and chemo-selectivity of hydroamination reaction (Table 3). Therefore, applying different solvents from polar, nonpolar, protic and aprotic was studied when complex (**1**) was used as a catalyst. Employing toluene as a nonpolar aprotic solvent, the higher yield was detected in comparison to polar aprotic solvents. The lower conversion in such solvent like DMF and acetonitrile is due to coordination of the solvent to Ru center and blocks the active catalytic sites of the complex. Using *n*-butanol as a solvent is not applicable due to the forming of some by-products from the *N*-alkylation reaction of amine in the presence of ruthenium catalyst. In this case, aniline takes part in another catalyst cycle and

**Table 3** Effect of different solvents on hydroamination of acrylonitrile with aniline

No	Solvent	Conversion (%) <sup>a</sup>	Selectivity <sup>b</sup>
1	DMF	50	88
2	Acetonitrile	45	90
3	<i>N</i> -butanol	20	–
4	Toluene	98	96
5	THF	87	95
6	Dioxane	50	83
7	No Solvent	50	87

Acrylonitrile (6 mmol), aniline (5 mmol), complex (**1**) (3 mol%),  $\text{K}_2\text{CO}_3$  (0.05 mmol), solvent (1 ml),  $T=100^\circ\text{C}$ , 20 h. **a** Data were determined by GC, and conversions were calculated for acrylonitrile using *n*-decane as standard **b** Selectivity is measured for Markovnikov product (Scheme 3)

**Table 2** Hydroamination of acrylonitrile with aniline in the presence of ruthenium  $\beta$ -diketiminate complexes

No	Complex	X	Y	Z	Conversion (%) <sup>a</sup>	Selectivity <sup>b</sup>
1	$[\text{Ru}(\text{p-cymen})\text{Cl}(\text{L}^{\text{H,Cl}})]$	H	Cl	H	98	95
2	$[\text{RuCl}(\text{L}^{\text{CH}_3, \text{H}})]$	$\text{CH}_3$	H	H	90	93
3	$[\text{Ru}(\text{C}_6\text{H}_6)\text{Cl}(\text{L}_\text{O}^{\text{CH}_3, \text{CH}_3})]$	$\text{CH}_3$	$\text{CH}_3$	H	83	92
4	$[\text{Ru}(\text{C}_6\text{H}_6)\text{Cl}(\text{L}_\text{O}^{\text{CF}_3, \text{CH}_3})]$	$\text{CF}_3$	$\text{CH}_3$	H	45	90
5	$[\text{Ru}(\text{C}_6\text{H}_6)\text{Cl}(\text{L}_\text{m}^{\text{CH}_3, \text{CH}_3})]$	$\text{CH}_3$	H	$\text{CH}_3$	80	90
6	$[\text{Ru}(\text{C}_6\text{H}_6)\text{Cl}(\text{L}_\text{m}^{\text{CH}_3, \text{CF}_3})]$	$\text{CH}_3$	H	$\text{CF}_3$	79	88

Acrylonitrile (6 mmol), aniline (5 mmol), catalyst (3 mol%),  $\text{K}_2\text{CO}_3$  (0.05 mmol), toluene (1 ml),  $T=100^\circ\text{C}$ , 20 h. **a** Data were determined by GC, and conversions were calculated for acrylonitrile using *n*-decane as standard **b** Selectivity is measured for Markovnikov product (scheme 3)

as a consequence conversion of styrene in the hydroamination reaction decreases [43] (Table 4).

There are numerous possibilities for the reaction pathway; one proposed mechanism is N–H bond activation. In the first step of this pathway, the N–H bond of amine binds to a coordinatively unsaturated ruthenium center giving the (amido) ruthenium hydride (Scheme 4). Then, alkene coordinates to the ruthenium center to form complex (2), followed by intramolecular nucleophilic attack of the nitrogen lone pair to the coordinated carbon–carbon double bond. Reductive elimination of alkylamido (3) would give the product (4) and reproduce the coordinatively unsaturated ruthenium center [44].

Encouraged by the results obtained with aniline, our attention turned to aliphatic amines, and as it was expected,

**Table 4** Catalytic hydroamination of different amines with acrylonitrile

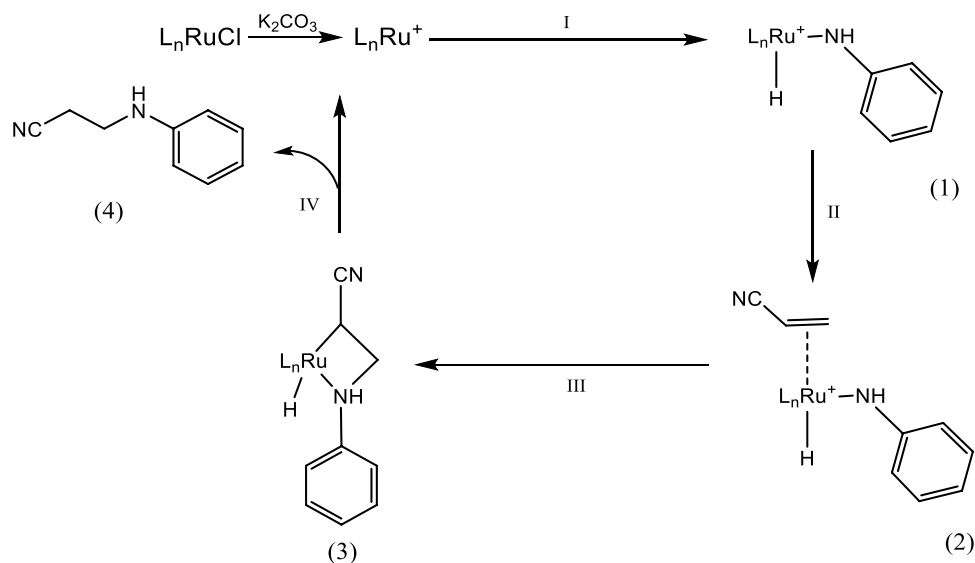
No	Amine	Conversion (%) <sup>b</sup>	Selectivity <sup>a</sup>
1	Cyclohexylamine	96	99
2	Hexylamine	99	99
3	Octylamine	99	99
4	Butylamine	99	99
5	Phenylethylamine	98	99
6	Morpholine	85	96
7	Diethylamine	82	97

Acrylonitrile (6 mmol), amine (5 mmol), [Ru(cymene)Cl<sub>2</sub>]<sub>2</sub> (3 mol%), dope (0.02 mmol), K<sub>2</sub>CO<sub>3</sub> (0.05 mmol), toluene (1 ml), T = 100 °C, 20 h.

<sup>a</sup>Data were determined by GC, and conversions were calculated for acrylonitrile using n-decane as standard

<sup>b</sup>Selectivity is measured for Markovnikov product (scheme 3)

**Scheme 4** Proposed mechanism for hydroamination of acrylonitrile with aniline leading to Markovnikov product



aliphatic amines show higher activity than aniline in hydroamination. The best results were obtained for primary amine (Table 5, entries 1–5). In comparison to primary alkyamines, secondary derivatives showed less activity, which is due to their higher nucleophilic property, as they coordinate more strongly to the metal, and their transfer to the carbon center is more difficult. In addition, the electrostatic repulsion between  $\pi$ -electrons of alkyne and more electron-rich secondary amines leads to greater steric effect.

## Crystal structure

The complex is air stable and soluble in most organic solvents. Suitable crystals of complex are obtained from mixture of dichloromethane and pentane in  $-30$  °C. Ortep view of complex is illustrated in Fig. 1, and the structure of complex is similar to previously reported ruthenium (II) complexes of  $\beta$ -diketimate [35]. The complex crystallized in the monoclinic space group P2(1)/c with four molecules in the unit cell. Single-crystal structure of this complex confirmed three-coordinate piano-stool geometry for Ru(II), with the ruthenium atom  $\pi$ -bonded to the p-cymene ring with an average Ru–C distance of 1.697 Å. The ruthenium atom is also directly coordinated to both nitrogen atoms of  $\beta$ -diketimate ligand with a normal distance of 2.119 and 2.121 Å.

Ru–Cl distances average is about 2.441 Å and is in agreement with the values reported for similar structure being the  $\eta^6$ -arene–Ru fragment in the CSD and similar structure. The complex folds along the N–N vector and the angle between the C<sub>6</sub>H<sub>6</sub> plane and the N1–C2–C11–C8–N2 plane is 83.8°. It seems that steric conflict between ortho-chloro N-aryl substituent and metal pushes the metal center out of the

**Table 5** Crystallographic and structure refinements data of complex [Ru(p-cymen)Cl(L<sup>H,Cl</sup>)]

Formula	C <sub>25</sub> H <sub>23</sub> Cl <sub>5</sub> N <sub>2</sub> Ru
Fw	629.77
$\lambda/\text{\AA}$	0.71073
T/K	100
crystal system	Monoclinic
space group	<i>P</i> 12 <sub>1</sub> / <i>c</i>
<i>a</i> / $\text{\AA}$	9.6509(5)
<i>b</i> / $\text{\AA}$	15.2380(8)
<i>c</i> / $\text{\AA}$	16.7019(8)
$\alpha/^\circ$	90
$\beta/^\circ$	93.167(2)
$\gamma/^\circ$	90
<i>V</i> / $\text{\AA}^3$	2452.4(2)
<i>D</i> <sub>calc</sub> /Mg.m <sup>-3</sup>	1.076
<i>Z</i>	4
$\mu$ (mm <sup>-1</sup> )	1.202
<i>F</i> (000)	1264.0
2 $\theta$ (°)	56.56
<i>R</i> (int)	0.0533
GOOF	1.027
<i>R</i> <sub>1</sub> <sup>a</sup> ( <i>I</i> > 2 $\sigma$ ( <i>I</i> ))	0.0283
<i>wR</i> <sub>2</sub> <sup>b</sup> ( <i>I</i> > 2 $\sigma$ ( <i>I</i> ))	0.0625
CCDC No	2,011,092

$$^a R_1 = \frac{\sum \|F_o\| - |F_c|}{\sum \|F_o\|}$$

$$^b wR_2 = \left[ \frac{\sum (w(F_o^2 - F_c^2)^2)}{\sum w(F_o^2)} \right]^{1/2}$$

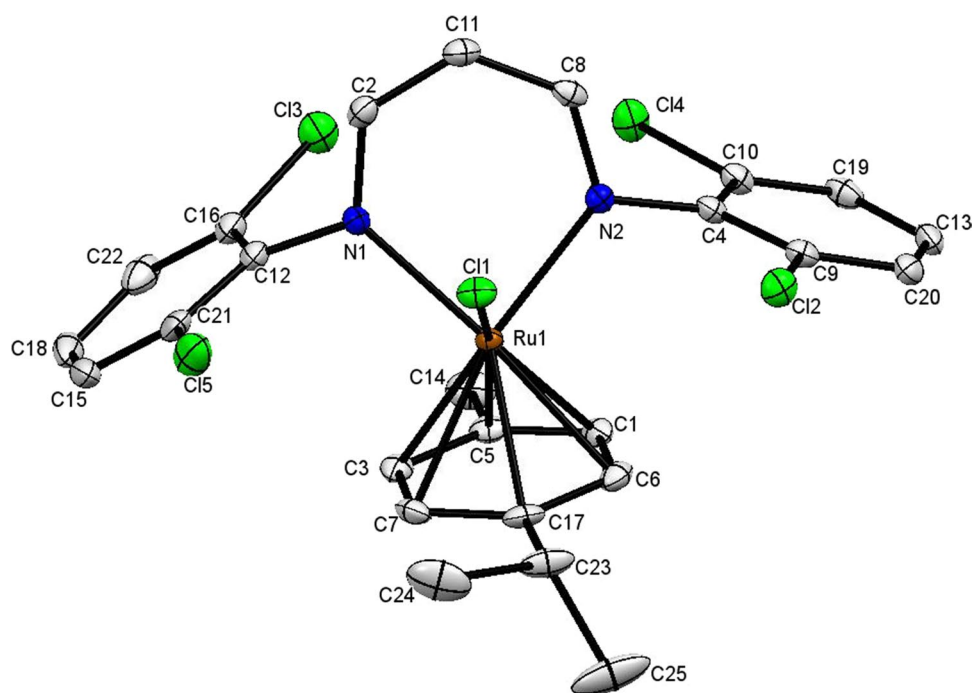
$\beta$ -diketiminato ligand plane. Some weak hydrogen bonds exist in the structure, stabilizing the packing of the complex; hydrogen bonds exist between the C–H bond in the flanking aryl groups and chloride ion of bonded to ruthenium center in the next molecule [C(18)<sup>ii</sup>–H(18)<sup>ii</sup>...Cl(1)<sup>i</sup>] = 2.704 Å, *i* = *x*, *y*, *z*, *ii* = 1 + *x*, *y*, *z* with an angle of 151.67 assembling a two-dimensional network. Furthermore, every asymmetric unit interacts with each other along *b* axis, via significant C–H... $\pi$  interaction between [C(1)–H(1)<sup>i</sup>...C<sub>centroid</sub>(C12–C21)<sup>iii</sup>] = 2.879 Å, *iii* = 1 – *x*, –1/2 + *y*, 1.5 – *z*. Crystallographic data for complex are listed in Table 5.

### Geometry optimization and quantum theory of atom in molecules

Full geometry optimization has been done using BP86 functional and the def2-TZVP basis sets. Geometry optimization was started from the single-crystal X-ray experimental atomic positions. Bond lengths and angles are in good agreement with their corresponding values from X-ray structural data. Figure 2 shows the superimposition of the calculated (DFT) and X-ray structure for the titled compound. It is notable that benzene ring positions are slightly different.

The QTAIM approach is repeatedly used for the bonding situation between the atoms [45, 46]. Here, this method is used in order to gain insight into binding characteristics of titled complex. QTAIM reveals interesting facts about hapticity and inter molecular interactions in titled complex. It can be seen that the central Ru is  $\eta^6$  and there are seven intermolecular Cl...H electrostatic interactions. Selected

**Fig. 1** Ortep view of complex (1), [Ru(cymene)Cl( $\beta$ -diketiminato)] for 50% ellipsoid



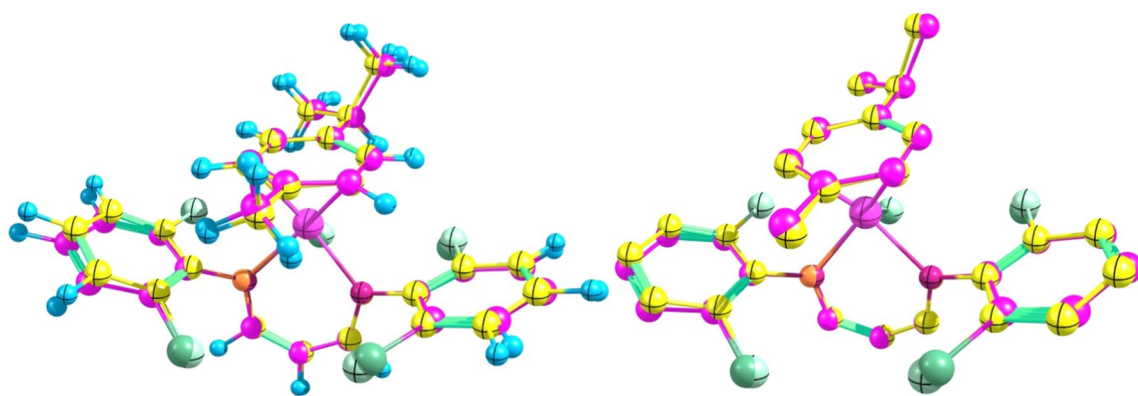


**Fig. 2** Atom-by-atom superimposition of the DFT-optimized compound on the X-ray structure

**Table 6** Bond critical point electron densities ( $\rho$ ), their Laplacian, ( $\nabla^2\rho$ ), ellipticities ( $\epsilon$ ) and Mayer bond order

Bond	Bond length <sub>Exp</sub>	Bond length <sub>Opt</sub>	$\rho$	$\nabla^2\rho$	$\epsilon$	Mayer B.O
Ru <sub>1</sub> –C <sub>9</sub>	2.182 (2)	2.193	0.088	0.224	0.66	0.57
Ru <sub>1</sub> –C <sub>17</sub>	2.195 (2)	2.206	0.082	0.268	0.55	0.46
Ru <sub>1</sub> –C <sub>37</sub>	2.224 (2)	2.244	0.083	0.214	1.11	0.45
Ru <sub>1</sub> –C <sub>19</sub>	2.217 (2)	2.220	0.079	0.258	1.19	0.43
Ru <sub>1</sub> –C <sub>13</sub>	2.207 (2)	2.191	0.084	0.218	0.66	0.56
Ru <sub>1</sub> –C <sub>16</sub>	2.241 (2)	2.266	0.081	0.241	0.67	0.33
Cl <sub>5</sub> ⋯Cl <sub>4</sub>	3.699 (2)	3.996	0.002	0.008	0.21	
Cl <sub>2</sub> ⋯Cl <sub>3</sub>	3.536 (2)	3.529	0.008	0.021	0.03	
Cl <sub>2</sub> ⋯Cl <sub>6</sub>	3.610 (2)	3.539	0.007	0.025	0.09	
C <sub>30</sub> –H <sub>31</sub> ⋯Cl <sub>4</sub>	2.9433 (6)	2.898	0.007	0.027	0.59	0.011
C <sub>30</sub> –H <sub>33</sub> ⋯Cl <sub>5</sub>	2.8592 (6)	2.950	0.008	0.025	0.65	0.038
C <sub>49</sub> –H <sub>50</sub> ⋯Cl <sub>2</sub>	2.7993 (5)	2.765	0.010	0.033	0.19	0.051
C <sub>49</sub> –H <sub>50</sub> ⋯Cl <sub>6</sub>	3.6440 (6)	3.522	0.003	0.010	0.23	0.003
C <sub>19</sub> –H <sub>20</sub> ⋯Cl <sub>6</sub>	3.0036 (6)	2.989	0.007	0.026	0.58	0.039
C <sub>47</sub> –H <sub>48</sub> ⋯Cl <sub>3</sub>	3.4717 (6)	3.318	0.003	0.009	0.20	0.006
C <sub>17</sub> –H <sub>18</sub> ⋯Cl <sub>3</sub>	2.9517 (6)	3.056	0.008	0.029	0.68	0.033

optimized geometric and QTAIM parameters are shown in Table 6 and Fig. 3.

### Frontier molecular orbitals

The frontier molecular orbitals (HOMO and LUMO) can reveal many properties of a compound. The iso-density plots for the HOMOs and LUMOs orbitals are shown in Fig. 4. It can be seen that HOMO is mainly localized on the metal atom and the ligand, while the LUMO is most on the benzene rings. By using HOMO and LUMO energy values for the molecule, electronegativity and chemical hardness can be calculated as follows:  $\chi = [(I + A)/2]$  (electronegativity),  $\eta = [(I - A)/2]$  (chemical hardness) where  $I$  and  $A$  are ionization potential and electron affinity;  $I = -E_{\text{HOMO}}$  and  $A = -E_{\text{LUMO}}$ , respectively [47, 48], and are reported in Table 7.

### Hirshfeld surface calculation

In order to gain better insight into the intermolecular interaction of molecular crystals, Hirshfeld surface [49, 50] and the related 2D fingerprint [51, 52] plot together with intermolecular interaction energies were calculated using Crystal Explorer [53]. Hirshfeld surface shows that the dominant interaction in the solid phase is two sets of Cl⋯H interactions between Cl connected to metal center and the C-H from neighboring molecule benzene ring (Figs. 5 and 6). The Hirshfeld surfaces mapped with  $d_{\text{norm}}$  for the complex and respected fingerprint plot are demonstrated in Fig. 7.

The dominant interaction in the complex is Cl-H can be seen in the Hirshfeld surface as the bright red areas. Intermolecular interaction energies for a 3.8 Å cluster are summarized in Table 8 and Fig. 6. Results suggest that the intermolecular interactions are of weak to moderate nature.

**Fig. 3** QTAIM molecular graph together with ball and stick

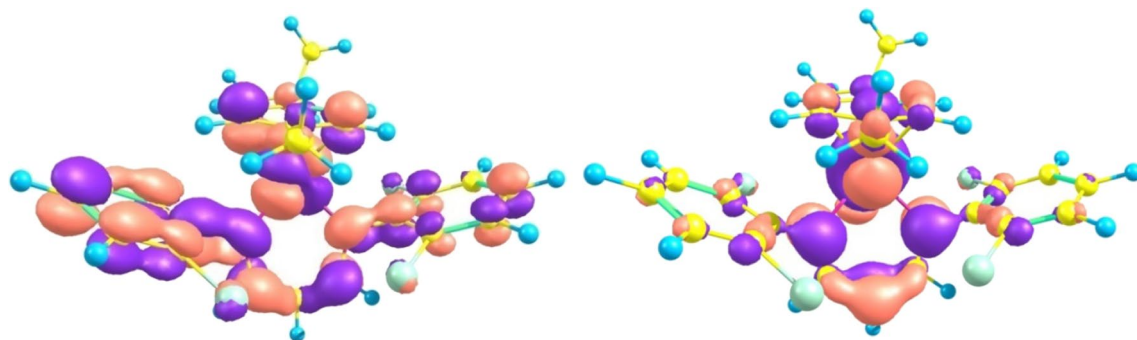
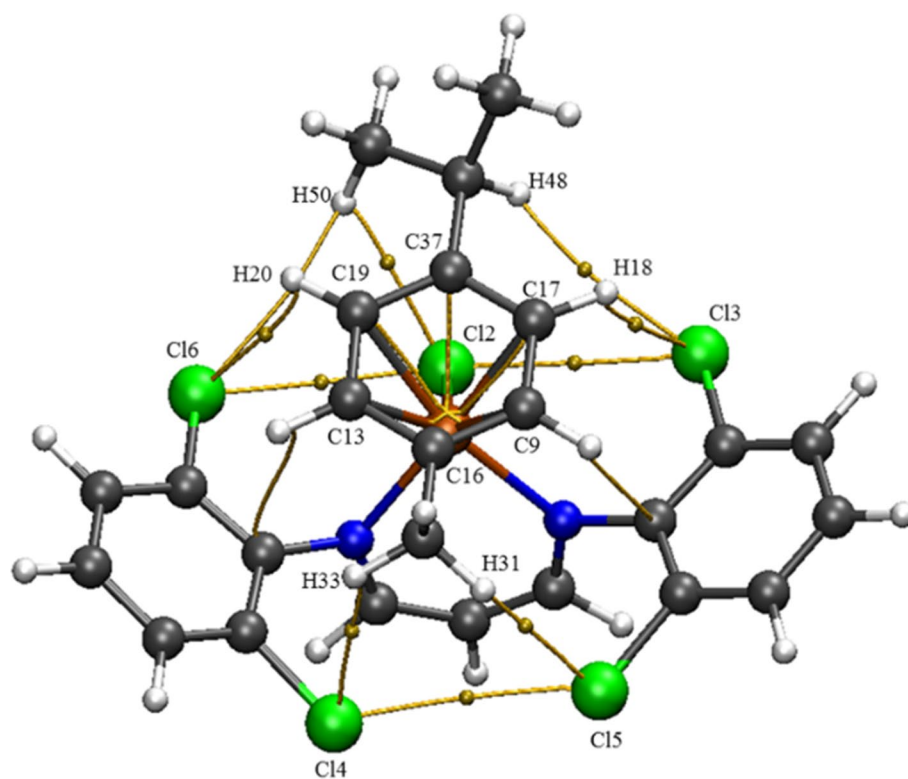


**Fig. 4** View of Frontier molecular orbitals LUMO (left) and HOMO (right)

**Table 7** Orbital energies, chemical hardness, chemical softness and electronegativity of complex [Ru(p-cymen)Cl(L<sup>H,Cl</sup>)]

B3P86 Def2-TZVP	
$E_{\text{HOMO}}$ (eV)	-4.35
$E_{\text{LUMO}}$ (eV)	-2.41
$\Delta E_{\text{HOMO-LUMO}}$	-1.94
Chemical hardness ( $\eta$ )	3.38
Chemical softness ( $S$ )	0.14
Electronegativity ( $\chi$ )	0.97

Two-dimensional fingerprint plots quantitatively summarize the nature and type of intermolecular contacts experienced by the molecules in the crystal. The Cl  $\cdots$  H/ H $\cdots$ Cl, H  $\cdots$  H/ H $\cdots$ H and C  $\cdots$  H/ H $\cdots$ C intermolecular interactions

appear as distinct spikes in the 2D, the fingerprint (Fig. 6). The amount of Cl  $\cdots$  H/ H $\cdots$ Cl interactions comprises 22.7% of the Hirshfeld surfaces.

## Conclusion

In this report, a new half-sandwich ruthenium (II) complex containing  $\beta$ -diketiminato ligand has been synthesized and it is found to efficiently catalyze the hydroamination of acrylonitrile with both anilines and aliphatic amines. The activity of complex was compared by a series of ruthenium  $\beta$ -diketiminato complexes, and it was shown that the electronic and steric environment of ligand have direct effect on

**Fig. 5** The three-dimensional Hirshfeld surface mapped with  $d_{\text{norm}}$  showing the intermolecular interactions

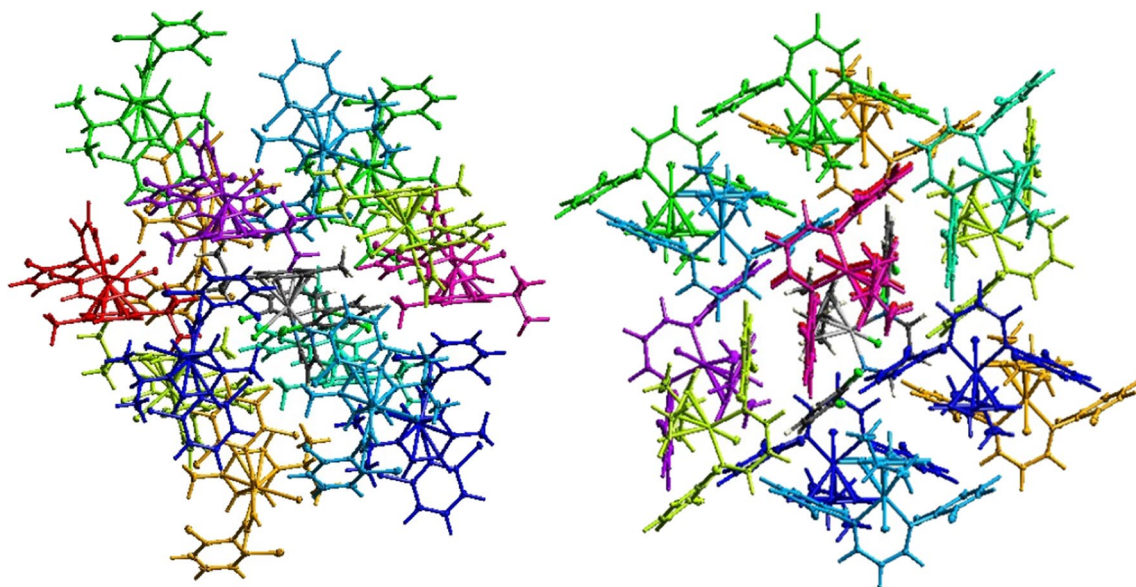
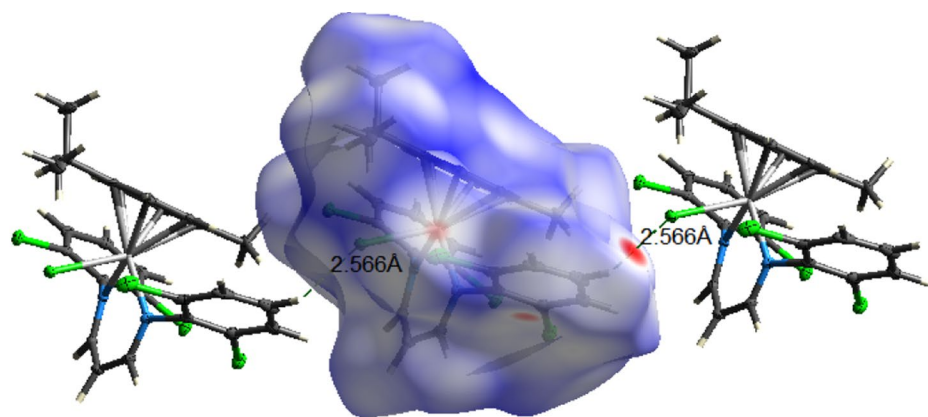


**Fig. 6** 3.8 Å radius cluster

activity of catalysts. The crystal structure of  $[\text{Ru}(\text{p-cymen})\text{Cl}(\text{L}^{\text{H,Cl}})]$  was determined by X-ray crystallographic analysis. DFT calculations together with QTAIM and Hirshfeld surfaces analysis reveal the Hapticity of the benzene ring

is 6 and  $\text{Cl}\cdots\text{H}$  is most dominant interaction in the titled compound. Comparative study of both experimental and theoretical values reveals that structural conformations are almost the same.

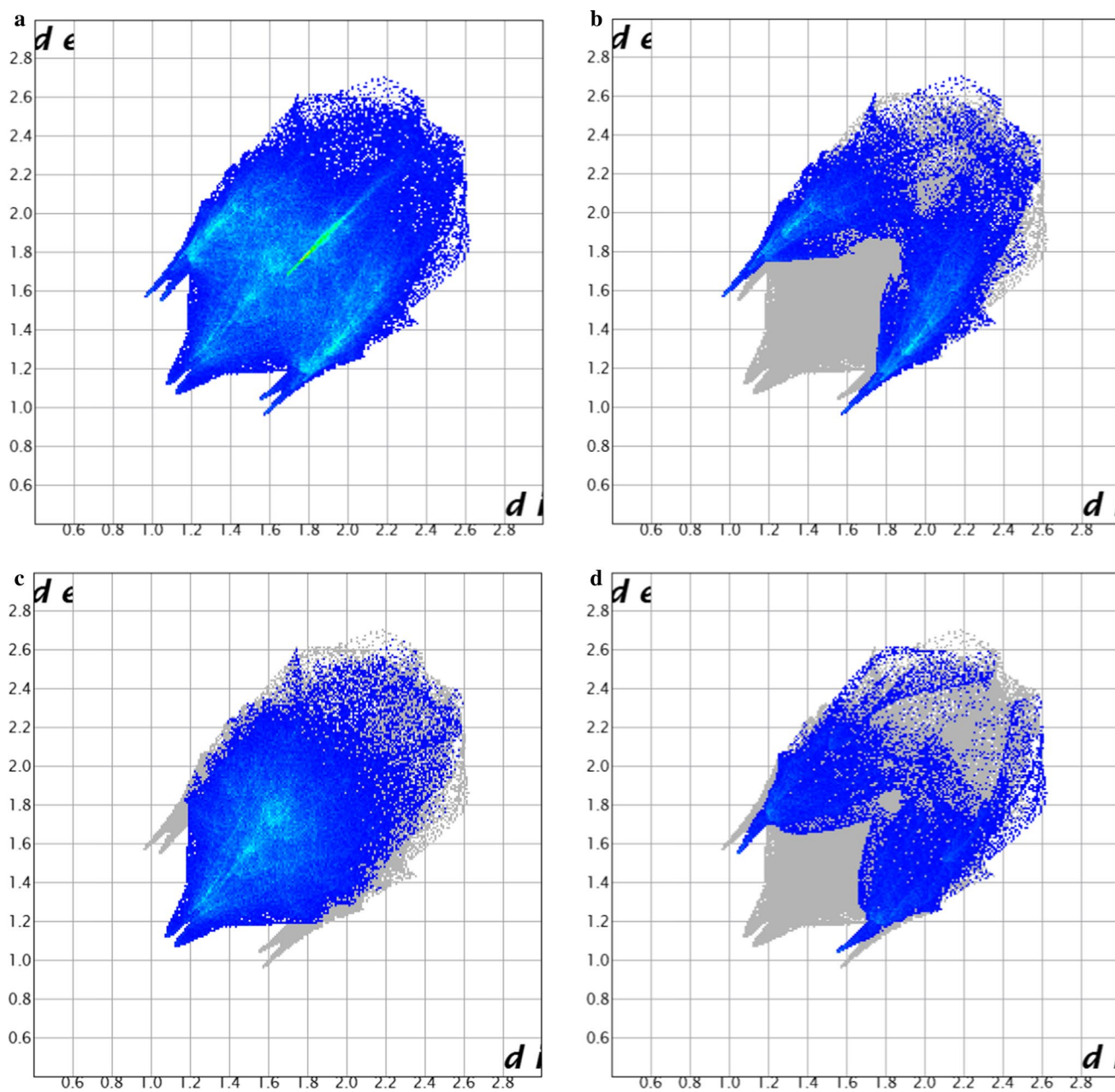


**Fig. 7** Two-dimensional fingerprint plots **a** all **b** Cl...H **c** H...H **d** C...H

**Table 8** Intermolecular interaction energies (kJ/mol) for a 3.8 Å cluster

N	Symop	$R^*$	Electron Density	$E_{ele}$	$E_{pol}$	$E_{dis}$	$E_{rep}$	$E_{tot}$
1	-x, -y, -z	10.33	HF/3-21G	-18.1	-9.8	-38.9	25.7	-39.1
2	-x, y+1/2, -z+1/2	9.69	HF/3-21G	-24.0	-11.7	-24.3	13.5	-43.0
1	x, y, z	9.65	HF/3-21G	-23.1	-12.6	-36.0	29.8	-40.0
1	x, -y+1/2, z+1/2	13.40	HF/3-21G	1.0	-0.3	-3.3	0.1	-2.1
0	-x, -y, -z	10.99	HF/3-21G	-5.2	-1.7	-35.8	15.0	-26.5
0	-x, y+1/2, -z+1/2	8.46	HF/3-21G	-12.1	-3.4	-64.2	36.8	-42.6
1	x, -y+1/2, z+1/2	9.61	HF/3-21G	-0.1	-2.7	-21.1	14.2	-9.4
1	-x, -y, -z	9.65	HF/3-21G	-4.1	-1.2	-38.8	14.9	-27.9
0	-x, -y, -z	9.46	HF/3-21G	-3.5	-2.1	-27.9	14.1	-18.6

## Supplementary data

CCDC number 2011092 contains the supplementary crystallographic data for  $C_{25}H_{23}Cl_5N_2Ru$  complex. These data can be obtained free of charge via <http://www.ccdc.cam.ac.uk>, or from the Cambridge Crystallographic Data Center, 12 Union Road, Cambridge CB2 1EZ, UK; Fax: +44 1223 336 033; or E-mail: [deposit@ccdc.cam.ac.uk](mailto:deposit@ccdc.cam.ac.uk).

**Acknowledgements** The authors gratefully acknowledge the financial support from Iran National Science Foundation (INSF).

## Compliance with ethical standards

**Conflict of interest** The authors declare that they have no conflict of interest.

## References

- Taylor RD, MacCoss M, Lawson AD (2014) *J Med Chem* 57:5845–5859
- Surry DS, Buchwald SL (2008) *Angew Chem Int Ed* 47:6338–6361
- Sapsford JS, Scott DJ, Allcock NJ, Fuchter MJ, Tighe CJ, Ashley AE (2018) *Adv Synth Catal* 360:1066–1071
- Fujita K-I, Enoki Y, Yamaguchi R (2008) *Tetrahedron* 64:1943–1954
- Kaloğlu N, Achard M, Bruneau C, Özdemir İ (2019) *Eur J Inorg Chem* 2019:2598–2606
- Huang L, Arndt M, Gooßen KT, Heydt H, Goossen LJ (2015) *Chem Rev* 115:2596–2697
- Muller TE, Hultzsck KC, Yus M, Foubelo F, Tada M (2008) *Chem Rev* 108:3795–3892
- Nishina N, Yamamoto Y (2012) *Late transition metal-catalyzed hydroamination. Hydrofunctionalization*. Springer, New York, pp 115–143
- Bernoud E, Lepori C, Mellah M, Schulz E, Hannedouche J (2015) *Catal Sci Technol* 5:2017–2037
- Martínez PH, Hultzsck KC, Hampel F (2006) *Chem Commun* 21:2221–2223
- Weitershaus K, Ward BD, Kubiak R, Müller C, Wadepohl H, Doye S, Gade LH (2009) *Dalton Trans* 23:4586–4602
- Ryu J-S, Li GY, Marks TJ (2003) *J Am Chem Soc* 125:12584–12605
- Li Y, Marks TJ (1996) *J Am Chem Soc* 118:9295–9306
- Gribkov DV, Hultzsck KC, Hampel F (2006) *J Am Chem Soc* 128:3748–3759
- Seayad J, Tillack A, Hartung CG, Beller M (2002) *Adv Synth Catal* 344:795–813
- Kozlov S (1936) *J Gen Chem USSR* 6:1341–1345
- Li K, Horton PN, Hursthouse MB, Hii KKM (2003) *J Organomet Chem* 665:250–257
- Fadini L, Togni A (2003) *Chem Commun* 1:30–31
- Hartung CG, Tillack A, Trauthwein H, Beller M (2001) *J Org Chem* 66:6339–6343
- Schaffrath H, Keim W (2001) *J Mol Catal A Chem* 168:9–14
- Hong SH, Chlenov A, Day MW, Grubbs RH (2007) *Angew Chem Int Ed* 46:5148–5151
- Trnka TM, Grubbs RH (2001) *Acc Chem Res* 34:18–29
- Burling S, Paine BM, Nama D, Brown VS, Mahon MF, Prior TJ, Pregosin PS, Whittlesey MK, Williams JM (2007) *J Am Chem Soc* 129:1987–1995
- Khan F-A, Vallat A, Süß-Fink G (2012) *J Mol Catal A Chem* 355:168–173
- Kumar P, Gupta RK, Pandey DS (2014) *Chem Soc Rev* 43:707–733
- Otsuka M, Yokoyama H, Endo K, Shibata T (2012) *Org Biomol Chem* 10:3815–3818
- Gök L, Türkmen H (2013) *Tetrahedron* 69:10669–10674
- Webster R (2017) *Dalton Trans* 46:4483–4498
- Shaffer DW, Ryken SA, Zarkesh RA, Heyduk AF (2012) *Inorg Chem* 51:12122–12131
- Tian X, Goddard R, Pörschke K-R (2006) *Organometallics* 25:5854–5862
- Fekl U, Goldberg KI (2003) *Adv Inorg Chem* 54:259–320
- Bernskoetter WH, Lobkovsky E, Chirik PJ (2005) *Organometallics* 24:6250–6259
- Phillips AD, Thommes K, Scopelliti R, Gandolfi C, Albrecht M, Severin K, Schreiber DF, Dyson PJ (2011) *Organometallics* 30:6119–6132
- Schreiber DF, Ortin Y, Müller-Bunz H, Phillips AD (2011) *Organometallics* 30:5381–5395
- Schreiber DF, O'Connor C, Grave C, Ortin Y, Müller-Bunz H, Phillips AD (2012) *ACS Catal* 2:2505–2511
- Neese F (2012) *Wiley Interdiscip Rev Comput Mol Sci* 2:73–78
- Lu T, Chen F (2012) *J Comput Chem* 33:580–592
- Hallman P, Stephenson T, Wilkinson G (1970) *Inorg Synth* 12:237–240
- Gilbert J, Wilkinson G (1969) *J Chem Soc A Inorg Phys Theor* 1749–1753
- Bennett M, Huang TN, Matheson T, Smith A, Ittel S, Nickerson W (1982) *Inorg Synth* 21:74–78
- Ahmad N, Levison J, Robinson S, Uttley M, Wonchoba E, Parshall G (1974) *Inorg Synth* 15:45–64
- Phillips AD, Zava O, Scopelliti R, Nazarov AA, Dyson PJ (2010) *Organometallics* 29:417–427
- Hamid MHS, Williams JM (2007) *Chem Commun* 725–727
- Uchamaru Y (1999) *Chem Commun* 1133–1134
- Bader R (1990) *Atoms in molecules (A quantum theory)*. Clarendon Press, Oxford
- Matta CF, Boyd RJ (2007) *The quantum theory of atoms in molecules: from solid state to DNA and drug design*
- Demircioğlu Z, Albayrak Ç, Büyükgüngör O (2014) *J Mol Struct* 1065:210–222
- Tanak H, Açar AA, Büyükgüngör O (2013) *J Mol Struct* 1048:41–50
- Spackman MA, Jayatilaka D (2009) *CrystEngComm* 11:19–32
- Clausen HF, Chevallier MS, Spackman MA, Iversen BB (2010) *New J Chem* 34:193–199
- Rohl AL, Moret M, Kaminsky W, Claborn K, McKinnon JJ, Kahr B (2008) *Cryst Growth Des* 8:4517–4525
- Parkin A, Barr G, Dong W, Gilmore CJ, Jayatilaka D, McKinnon JJ, Spackman MA, Wilson CC (2007) *CrystEngComm* 9:648–652
- S. Wolff, D. Grimwood, J. McKinnon, M. Turner, D. Jayatilaka, M. Spackman, in: University of Western Australia Crawley, Australia, 2012.
- Mackenzie CF, Spackman PR, Jayatilaka D, Spackman MA (2017) *IUCrJ* 4:575–587

**Publisher's Note** Springer Nature remains neutral with regard to jurisdictional claims in published maps and institutional affiliations.